



Examination of the effect of the reactive power control of photovoltaic systems on electric power grids and the development of a voltage-regulation method that considers feeder impedance sensitivity

Insu Kim^{a,*}, Ronald G. Harley^{b,c}

^a Electrical Engineering, Inha University, Incheon, 22212, South Korea

^b Electrical and Computer Engineering, Georgia Institute of Technology, Atlanta, GA 30332, USA

^c Professor Emeritus at the University of KwaZulu-Natal, Durban, South Africa

ARTICLE INFO

Keywords:

Distributed generation (DG)
Photovoltaic (PV) systems
Reactive power control
OpenDSS
Volt/Var control

ABSTRACT

When relatively high-capacity renewable photovoltaic (PV) systems are connected to a grid, they can increase or decrease the voltage along feeders because of reverse power flow, even exceeding \pm five percent of the rated voltage. Nowadays, grid-connected inverter-based PV systems that can control reactive power can alleviate such an increase or decrease in voltage by adjusting the reactive power, which is referred to as Volt/Var control and management. Therefore, the objective of this paper is to (a) perform case studies to analyze the steady-state response of a large distribution network (i.e., with more than 1000 buses) with high-capacity PV systems that can control Volt/Var (i.e., either producing or consuming reactive power) and (b) present a Volt/Var-control method for three-phase voltage regulation that uses the positive-sequence sensitivity impedance matrix with power-factor constraints. This method is verified in the IEEE 34-bus test feeder. Thus, the proposed methods can be used to regulate the voltage of a bus to which a PV system is connected if the system controls reactive power. These proposed methods can also be used for various impact studies for the operation or planning of distribution systems with such PV systems.

1. Introduction

Photovoltaic (PV) systems with a capacity from tens to thousands of kW that are connected to a distribution network below 30 kV can reduce losses and daytime peak demand, which is known as peak load shaving. However, if these systems are not adequately regulated, they can increase or decrease the voltage because of reverse power flow. Thanks to inverters that can control reactive power, modern inverter-based PV systems that are connected to grids can actively control reactive power, which is referred to as Volt/Var control and management. However, the connection of such PV systems to grids requires mutually well-coordinated voltage-regulation agreements between utilities and PV owners (or PV operators) if the PV systems regulate voltage. In fact, variations in the power output from PV systems can be regulated by utilities so that the feeder voltage can be maintained within a set range of the rated voltage (i.e., ANSI C84.1–2016 Range A [1] or EN 50160 [2]). In addition to voltage regulation, a distribution network that hosts PV systems should be able to detect abnormal or limited conditions according to the voltage ranges and clearing times, as presented in

[3,4]. Furthermore, settings for dynamic or static voltage regulation can be allowed only under mutual agreement between PV owners and utilities [3,4].

Many studies examined the steady-state response of distribution networks that are enhanced by grid-connected PV systems (with the unity power factor). The most well-known benefit of using distributed generation (DG), particularly PV in this study, is peak load shaving [5,6]. One study claimed that utility distribution systems would experience a substantial increase in DG systems over the following few decades and addressed issues regarding changes (i.e., overcurrent protection conflicts during operation with DG, instantaneous reclosing, improved reliability from installing DG, and transformer connections) [7,8]. Another study examined reverse power flow, voltage rise and fluctuations, and reactive power fluctuations that are caused by grid-connected PV systems during the steady state [9]. Furthermore, an analytical method that was based on voltage sensitivity analysis for a linearized power system model was proposed in [10]. Then, the maximum limits of acceptable power that a DG system could inject while not violating five percent of the rated voltage at the steady state were

* Corresponding author.

E-mail address: insu@inha.ac.kr (I. Kim).

Nomenclature

CVR	conservation voltage regulation
DG	distributed generation
$\delta_{v,a,i}^{(j)}$	voltage angle of phase a for the i th bus at the j th iteration
EPRI	Electric Power Research Institute
$\Delta \mathbf{I}_{q,i}^{(0)}$	quadrature current of phases a , b , and c for the i th bus at the j th iteration
N	total number of buses
OpenDSS	Open Distribution System Simulator
P	active power
P_{DG}	active power output of a DG system
P_f	power-factor limit of a bus (e.g., either a leading or lagging power factor of 0.9 or higher)
p.u.	per unit

PV	photovoltaic
Q	reactive power
Q_{DG}	reactive power output of a DG system
$\text{Sign}(x)$	+1 if $x > 0$, $\text{Sign}(x) = 0$ if $x = 0$, or $\text{Sign}(x) = -1$ if $x < 0$
S_{nom}	nameplate capacity of a DG system
\mathbf{T}	$1/3 \times [1 \ 1 \ 1; 1 \ \alpha \ 2; 1 \ \alpha \ 2]$ and $\alpha = 1 \angle 120^\circ$
V	voltage
$V_i^{pos,(j)}$	positive-sequence voltage of the i th bus at the j th iteration
$V_{set,i}^{pos}$	positive-sequence set voltage magnitude of the i th bus in p.u.
\mathbf{Z}_{abc}	3×3 phase impedance matrix
\mathbf{Z}_{bus}	three-phase sensitivity impedance matrix
$Z_{bus,i}^{pos}$	i th diagonal term of the positive-sequence sensitivity impedance matrix

determined in [10]. A probabilistic power-flow method that was based on time-series and quasi-sequential Monte Carlo simulations also examined the effect of grid-connected PV systems on voltage in [11,12]. These studies indicated that voltage fluctuations from PV systems with relatively low capacity could be limited [13].

However, these previous studies only examined relatively low-capacity DG systems. Another study investigated the effects of PV systems with penetration levels of 10, 30, and 50% on voltage, tap changes of regulators, and losses of the system and claimed that existing control settings for regulators and capacitor banks on feeders that were enhanced by high-penetration PV systems (50%) failed to mitigate voltage increases [14]. Thus, several studies presented a bi-level control framework of large-scale DG systems [15] and a multi-agent-based load-management method [16]. Then, another recent study claimed that the maximum penetration level of distributed PV systems (which do not violate the voltage limits) could be 50% and that of clustered PV systems could be 30% [17]. Because of Monte Carlo and unbalanced power-flow simulations, indirect voltage support was possible by combining high-capacity PV (i.e., up to 100% of PV penetration) and energy-storage systems [18].

While these previous studies also analyzed PV systems that could not control reactive power, one study proposed a reactive power-control method that would not increase the voltage [19]. Furthermore, a study used the Open Distribution System Simulator (OpenDSS) and calculated the time-series steady-state power flow of a test feeder that was enhanced by PV systems with a capacity of 20% of the peak demand to control Volt/Var. This study concluded that PV inverters with an appropriate reactive power-control function could increase the hosting capacity (i.e., the allowable maximum capacity) of DG systems without creating voltage fluctuations [20,21]. Another study modeled grid-connected inverters for PV systems that could control Volt/Var, Volt/Watt, and dynamic reactive power [22]. One study also showed that a voltage-instability problem could be mitigated by PV inverters that could control reactive power after analyzing an IEEE 13-bus feeder that was integrated with PV systems [23]. The reactive power control of high-capacity PV systems could also improve the performance of control systems [24].

Because previous studies did not optimally control reactive power, some studies presented various optimal Volt/Var-control methods and algorithms [25–27] and active power-control methods [28–32]. Moreover, DG systems that could control reactive power were optimally allocated in [33–36]. However, these previous studies did not perform the steady-state analysis of large-distribution feeders with more than 1000 buses, which were enhanced by relatively high-capacity PV systems (i.e., 30%) that could control Volt/Var at high resolution (i.e., 15-min intervals). Furthermore, none of these previous studies presented a three-phase Volt/Var method that used the positive-sequence sensitivity impedance matrix with power-factor constraints for unbalanced

distribution networks. The proposed method can consider feeder impedance sensitivity during voltage regulation.

The proposed Volt/Var-control algorithm can be used for the local feedback controller of DG (including PV) inverters, which should maintain their bus voltage within a set voltage range by controlling reactive power. Moreover, the proposed methods can examine the maximum effect of DG systems by controlling reactive power during voltage regulation. These proposed methods are also verified in heavily unbalanced three-phase systems and, thus, are applicable to unbalanced systems and various three-phase power-flow analysis programs (e.g., DigSILENT and OpenDSS). The proposed pseudo codes that build a three-phase sensitivity impedance matrix can also be used for other research purposes.

This paper is organized as follows. Section 3 presents the problem statement. Section 4 provides a case study that analyzes the steady-state response of a large distribution network. Section 5 proposes a Volt/Var-control method for three-phase voltage regulation. Section 6 summarizes the major conclusions of this study.

2. Problem statement

The objective of this study is to (a) perform case studies to analyze the steady-state response of a large distribution network when relatively moderate- and high-capacity renewable PV systems participate in reactive-power control and (b) present a Volt/Var-control method for three-phase voltage regulation. First, this study models a substation distribution system, which includes feeder J1 with 3434 buses and hosts thirteen PV systems [37], by using OpenDSS for steady-state power-flow analysis [38]. Then, this paper calculates the steady-state power-flow of the distribution system during a week at 15-min intervals when the PV systems control reactive power. Next, this study analyzes an increase in overvoltage from active and reactive power that is produced by grid-connected PV systems and the effect of Volt/Var control on such an increase in voltage. The reactive power output that is calculated in the case study is determined by the predefined Volt/Var

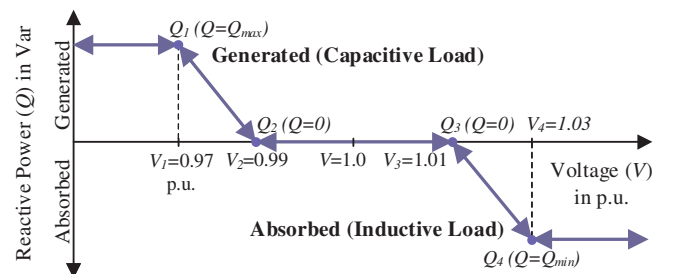


Fig. 1. Example of Volt/Var control [35].

Table 1
Substation distribution system, including feeder J1 [40].

Feeders	J1 and an aggregate load feeder
Number of buses (nodes)	3434 (4245)
Total peak generation (peak)	11.61 MW (9.39 MW)
Nominal voltages	12.47 and 0.416 kV (line-to-line)
Location	Northeastern United States
Customer type	Residential, commercial, and light industrial
Load model	Linear P (CVR P = 0.8) and quadratic Q (CVR Q = 3) load model in OpenDSS
Number of total loads	1,384
Total length	58 miles of primary lines
PV systems	2.0 MVA ($\approx 1813.6 \text{ kW} = 15.6\%$ of 11.61 MW) and 4.0 MVA (31.2% of 11.61 MW)

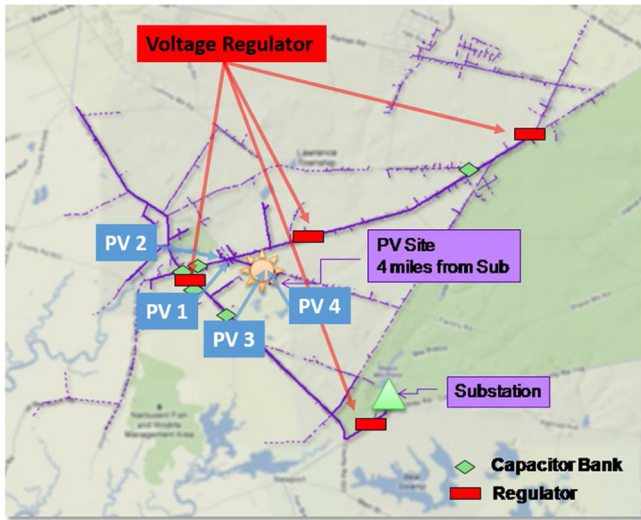


Fig. 2. Large distribution system, including feeder J1, in the northeastern United States [37,40].

- (a) Without PV systems.
- (b) With PV systems that cannot control Volt/Var.

Table 2
Set points of inverters that can control Volt/Var.

PV bus voltage (V)		Reactive power (Q)
Base voltage of 120 V	p.u.	p.u.
114	0.9500	$Q_{max} = +0.4$ (= Q_1 in Fig. 1)
119 [20]	0.9917 [20]	$Q_2 = 0$
121 [20]	1.0083 [20]	$Q_3 = 0$
126	1.0500	$Q_{min} = -0.4$ (= Q_4 in Fig. 1)

slope, so the reactive power may not maintain voltage within a set voltage range. However, the second case study proposes a three-phase Volt/Var-control method that can regulate positive-sequence voltage with power-factor constraints or active and reactive power constraints. The proposed method considers feeder impedance sensitivity, which is verified by the IEEE 34-bus test feeder.

3. Reactive power control

3.1. Steady-state operation of a PV inverter

Current grid-connected DG systems should maintain the terminal voltage of a bus to which they are connected within a set range of the rated voltage, typically within \pm five percent [39] or \pm ten percent [2]. To maintain a terminal voltage from 0.95 to 1.05 p.u., modern inverter-based DG systems that are connected to a grid, particularly PV

systems in this study, can control reactive power under the mutual agreement of local utilities and the PV operator under limited or planned conditions. That is, these systems can either consume or inject reactive power in the grid. Fig. 1 presents the reactive power control of an inverter that maintains its terminal voltage within a range from 0.99 p.u. and 1.01 p.u. If the range of a bus’s terminal voltage decreases below V_2 (i.e., 0.99 p.u.), the inverter produces reactive power within the grid, functioning as a capacitor. On the contrary, if the terminal voltage increases above V_3 (i.e., 1.01 p.u.), the inverter consumes reactive power, functioning as an inductor [35]. If its terminal voltage ranges between 0.99 and 1.01 p.u., the inverter produces only active power.

The Volt/Var control method in Fig. 1 can be characterized by

$$Q(V) = \begin{cases} Q_{max} & V \leq V_1 \\ \frac{(V_2 - V)}{V_2 - V_1} Q_{max} & V_1 \leq V \leq V_2 \\ 0 & V_2 \leq V \leq V_3 \\ \frac{(V_3 - V)}{V_3 - V_4} Q_{min} & V_3 \leq V \leq V_4 \\ Q_{min} & V_4 \leq V \end{cases} \quad (1)$$

3.2. Volt/Var control in a large distribution system

Large distribution systems, including the feeders J1, K1, and M1, have been published on the public domain website of the Electric Power Research Institute (EPRI) for research purposes [37]. By using OpenDSS, this study initially models a substation distribution system, including feeder J1 and thirteen PV systems that can control Volt/Var, as presented in Fig. 1 and Eq. (1). The detailed specifications of the substation, including feeder J1, are presented in Table 1 [37,40]. The distribution system has highly unbalanced local loads of 9.39 MW at a line-to-neutral voltage of 0.24 kV, a total power generation of 11.61 MW at this peak load, and thirteen PV systems. This study also models four three-phase PV systems with a total capacity of 1882 kVA, as shown in Fig. 2, and nine single-phase PV systems with a total capacity of 114 kVA, which are scattered throughout the distribution system. Inverters in PV systems can control reactive power based on the proposed control strategy in Fig. 1. Table 2 presents the set points of the inverter. The minimum and maximum reactive powers (Q_{min} of -0.4 p.u. and Q_{max} of $+0.4$ p.u.) are selected to maintain a lagging or leading power factor of 0.9 or higher [41].

3.2.1. Effect of PV systems without Volt/Var control

The reverse current that flows from grid-connected PV systems reduces the daytime peak load, which is known as peak load shaving [5,6], if the storage or any other systems are not combined. However, the PV systems can also increase the voltage of a bus to which the PV systems are connected. To examine the effect of PV systems that cannot control Volt/Var on increases in voltage, this study initially calculates the power flow of the distribution system that hosts the thirteen PV systems with relatively moderate capacity, or 15.6% of the peak power generation of the distribution system. The power-flow calculation only considers the peak generation of a distribution system with PV systems that cannot control Volt/Var to produce their assumed maximum full power. Fig. 3 plots the voltage along the feeder of the distribution system that produces its peak power, or 11.61 MW, with the distance from the incoming feeder. That is, the PV systems in Fig. 3(a) are not available. However, in Fig. 3(b), PV systems with a capacity of 15.6% of the peak power are available. In both the voltages along the feeder, the voltage regulators at distances of 5, 8, and 13 km from the incoming feeder significantly increase the voltage. Fig. 3(a) indicates that all the voltages occur within a range of \pm 5% of the rated voltage. However, in Fig. 3(b), the reverse current that flows from the grid-connected PV systems increases the feeder voltage.

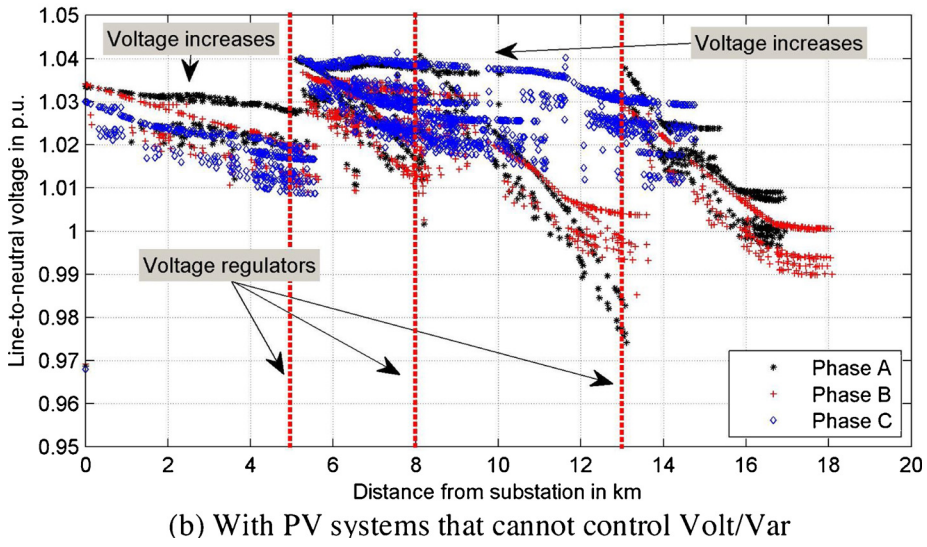
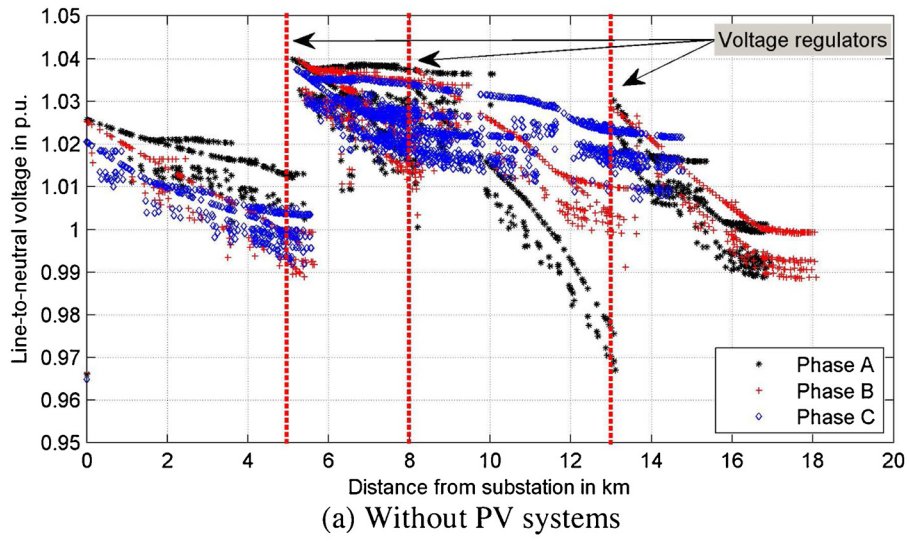


Fig. 3. Voltage along the feeder.

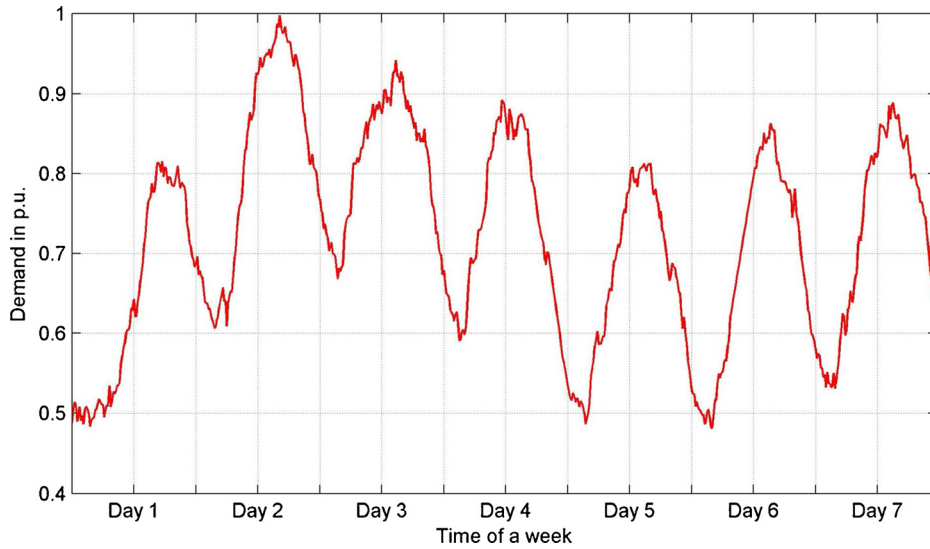


Fig. 4. Demand profile over a week in 15-min intervals.

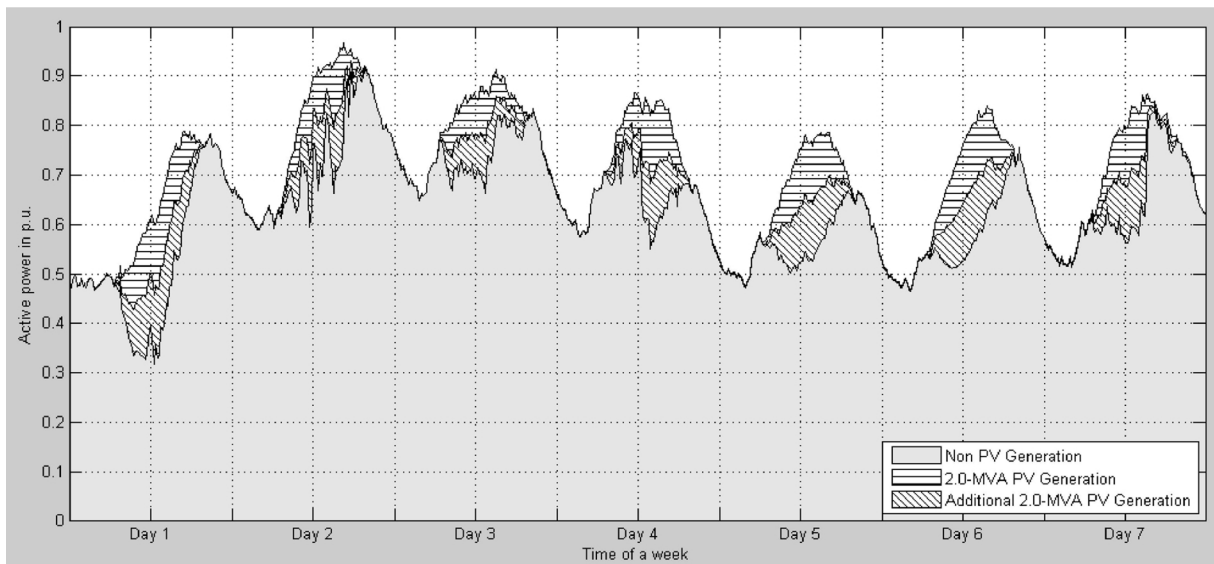


Fig. 5. Weekly active power output produced by the PV systems (at a base of 11.916 MVA).

(a) PV systems that cannot control Volt/Var.

(b) PV systems that can control Volt/Var.

3.2.2. Time-series power-flow calculation

Solar-irradiance input to PV panels always shows variability because of various weather conditions (e.g., overcast, heavily shaded, or sunny days because of rain, snow, ice, hail, transient cloudiness, and weather disturbances). Therefore, the actual generation output of PV systems is collected from the measurement data in [37], the period of which is a week in 15-min intervals from June 17 to June 25, 2012. These data are used as input data for steady-state power-flow calculation. In addition to variations in PV-generation output, the generation output of a distribution system varies according to continuously varying customer demands. Therefore, the load profile data in Fig. 4 are collected from [42], ranging from Sunday to Saturday in 15-min intervals at a peak of 9.39 MW and a load factor of 0.73. These data are also used as input data for steady-state power-flow calculation.

As an example of PV systems with relatively high capacity, additional thirteen PV systems with a total capacity of 15.6% of the peak power are added to the same locations as the existing thirteen PV systems. Thus, the PV systems have a total capacity of 31.2% of the peak power. Fig. 5 shows a weekly generation profile. The horizontally dashed areas, which are labeled as “2-MVA PV Generation,” correspond to the active power output that is generated by the thirteen PV systems with a total capacity of 15.6% of the peak power. The diagonally dashed areas, which are labeled as “Additional 2-MVA PV Generation,” correspond to the active power output that is produced by the additional thirteen PV systems as an example of relatively high-capacity PV systems. The PV systems operate at a power factor of unity; that is, they produce only active power. Fig. 5 reveals that relatively moderate- and high-capacity PV systems that inject active power to the grid effectively reduce the daytime peak load, which can be treated as a validation of the proposed time-series power-flow calculation case study.

3.2.3. Effect of PV systems that can control Volt/Var

Reverse power that flows from grid-connected PV systems, which reduces the peak load, can increase overvoltage. Thus, this study examines the maximum voltages of the distribution system during the week. The maximum feeder voltages for the active power output from high-capacity PV systems (i.e., 31.2% of the peak power of the distribution system) that cannot control Volt/Var are plotted in Fig. 6(a). In this figure, the high-capacity PV systems that cannot control Volt/Var, which are labeled as “4-MVA PV”, increase the voltage. In particular, approximately seventeen data points exceed 1.045 p.u. for “4-

MVA PV.” In Fig. 6(b), the maximum voltages show a stable pattern despite increased PV generation because the PV systems control reactive power.

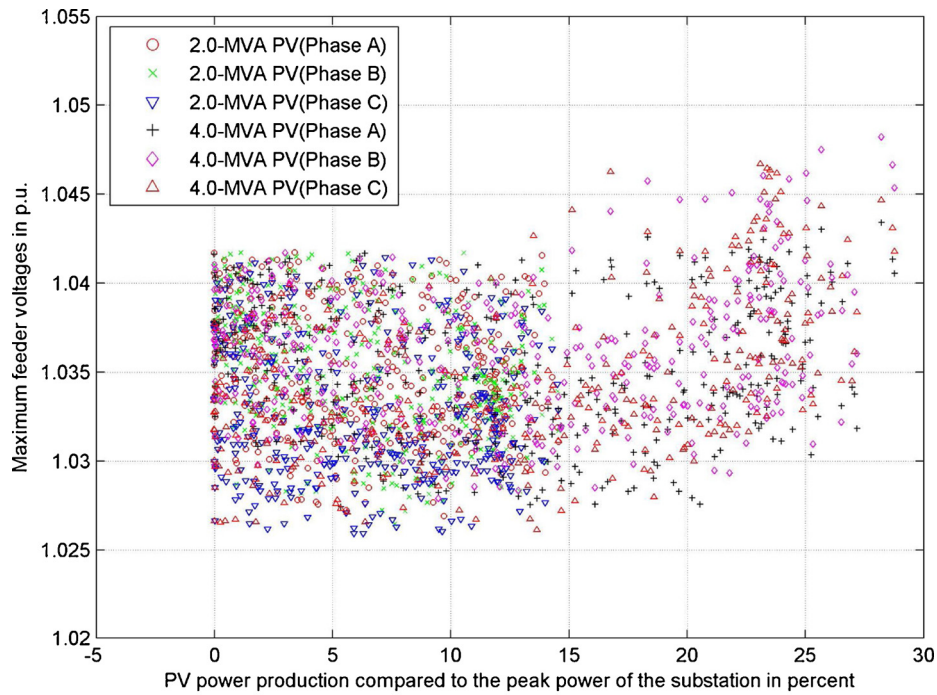
Fig. 7 indicates the feeder voltage of phase A in bus 5890628219, to which the largest-capacity PV system (i.e., 1672 kVA) is connected, on the 5th day. Without any PV systems, which is labeled as “No PV” and plotted by the solid black line, the feeder voltage does not exceed the upper limit of 1.05 p.u. However, with a PV system that produces only active power, which is labeled as “PV without V/V” and plotted by the thin dash-dotted blue line, the feeder voltage rises close to 1.04 p.u. at noon. With a PV system that controls reactive power, which is labeled as “PV with V/V” and plotted by the thick dashed red line, the feeder voltage is regulated between 1.01 p.u. and 1.025 p.u. In fact, Figs. 6 and 7 reveal that the PV systems that can control reactive power can exhibit less variation from 1.0 p.u., particularly by absorbing reactive power in this case.

Fig. 8 presents the reactive power at the slack bus, i.e., the substation’s incoming feeder header. With PV systems that cannot control the reactive power, which is plotted by the thin dash-dotted blue line, the active and reactive power at the slack bus decrease because of the peak-load reduction compared to the case without PV systems, which is plotted by the thin solid black line. However, with PV systems that can control the reactive power, which is plotted by the thick dashed red line, many buses in the test feeder experience an increase in the voltage (i.e., higher than 1.0 p.u.), so the PV inverters consume the reactive power to decrease the bus voltage. Thus, the reactive power at the slack bus increases by as much as the amount of reactive power that is absorbed by the PV inverters.

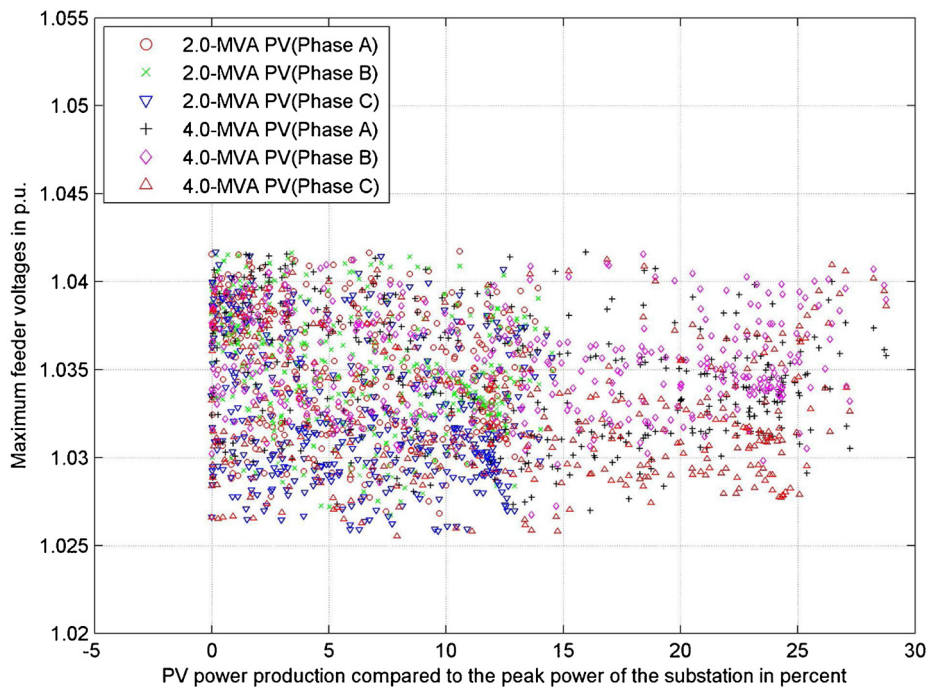
4. Volt/Var control

4.1. Iterative voltage regulation

Fig. 1 and Eq. (1) indicate that the inverter can regulate the voltage by either consuming or producing reactive power if the current bus voltage is measured. That is, the voltage of a bus to which a DG system is connected can be maintained within the set voltage range. However, in Eq. (1), the reactive power is determined by the relationship between the predefined slope and the voltage’s current magnitude. That is, Fig. 1 and Eq. (1) do not consider the impedance sensitivity of the feeders. In [43], the positive-sequence voltage control method could regulate the



(a) PV systems that cannot control Volt/Var



(b) PV systems that can control Volt/Var

Fig. 6. Maximum feeder voltages of the test feeder.

average magnitude of the three-phase voltages. However [43], did not present a method that could find the feeder sensitivity impedance or apply power-factor constraints to regulate the voltage’s magnitude. Therefore, this study proposes the following three-phase Volt/Var-control method that regulates the positive-sequence voltage with power-factor constraints.

The positive-sequence voltage mismatch between the set voltage

and the voltage at the current iteration is initially determined by

$$\Delta V_i^{pos,(j)} = V_{set,i}^{pos} - |V_i^{pos,(j)}|. \tag{2}$$

Then, the magnitude of the quadrature current is determined by the real, imaginary, or absolute value of the positive-sequence sensitivity impedance matrix, the detailed building methods of which will be presented in the next section.

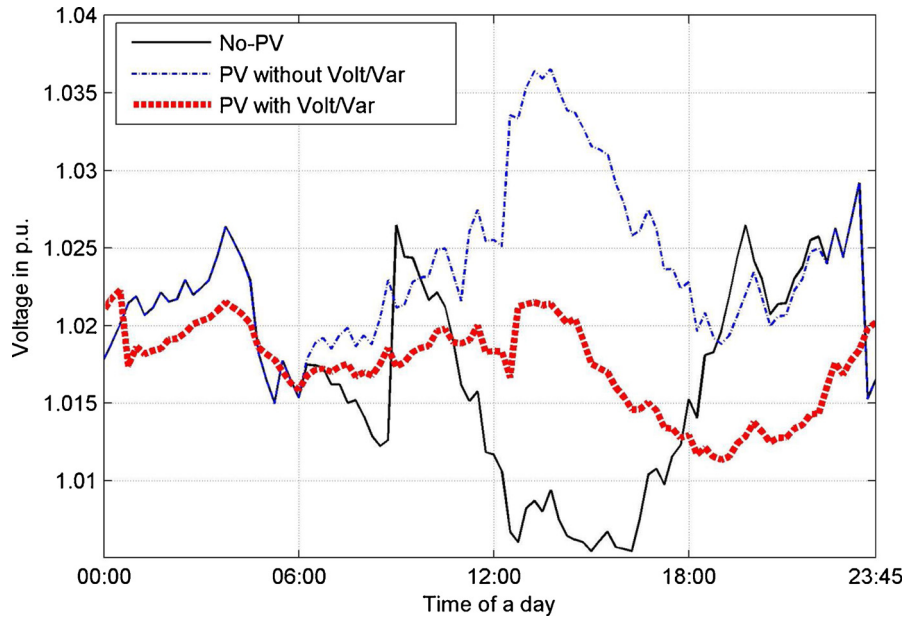


Fig. 7. Voltage of phase A in bus 5890628219, which hosts the largest PV system (5th day).

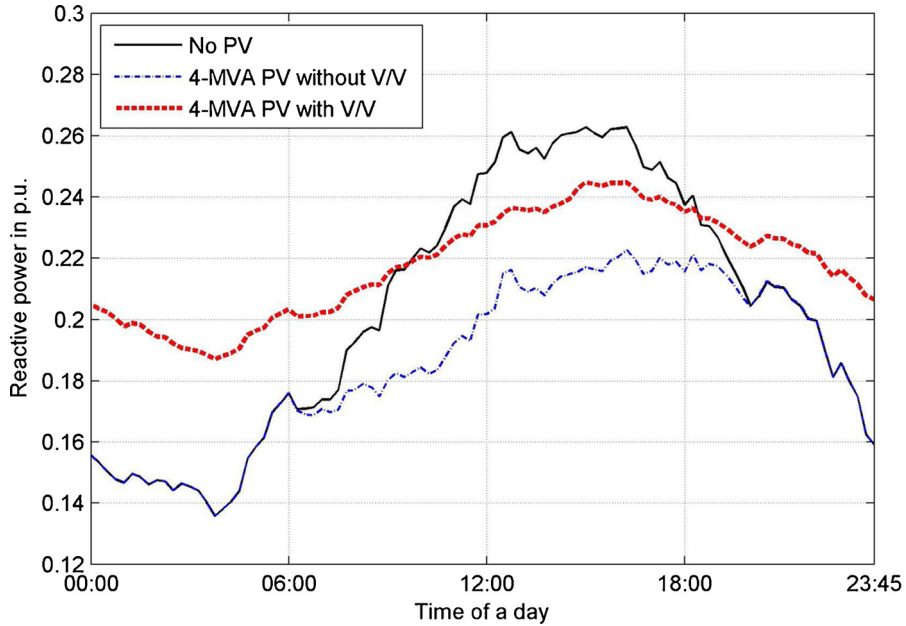


Fig. 8. Reactive power at the slack bus, or the substation feeder header.

Table 3

Pseudo code 1. Finding a bus that is connected to the reference.

```

nbr := no. of branches
for i := 1 to nbr
  j := starting bus, k := ending bus, and id := phase impedance matrix id
  if j == 0
    zb := Zabc((id-1)×3+1:id×3, 1:3)
    Zbus((k-1)×3+1:k×3, (k-1)×3+1:k×3) := zb
  end
end
end
    
```

$$|\Delta I_{q,i}^{(j)}| \approx \frac{\Delta V_i^{pos,(j)}}{|Z_{bus,i}^{pos}|}. \quad (3)$$

The proposed method is based on three phases, so the quadrature current of each phase is determined by

$$\Delta \mathbf{I}_{q,i}^{(j)} = \Delta \mathbf{I}_{q,i}^{(j-1)} + \begin{bmatrix} |\Delta I_{q,i}^{(j)}| \angle (\text{Sign}(\Delta V_i^{pos,(j)}) \times 90^\circ + \delta_{V_{a,i}^{(j)}}) \\ |\Delta I_{q,i}^{(j)}| \angle (\text{Sign}(\Delta V_i^{pos,(j)}) \times 90^\circ + \delta_{V_{b,i}^{(j)}}) \\ |\Delta I_{q,i}^{(j)}| \angle (\text{Sign}(\Delta V_i^{pos,(j)}) \times 90^\circ + \delta_{V_{c,i}^{(j)}}) \end{bmatrix}. \quad (4)$$

Then, the proposed method iterates Eqs. (2) to (4) until convergence is achieved. The following constraints are also included to avoid exceeding the limit of the reactive power output:

$$\{0, -pf \times S_{nom}\} \leq P_{DG} \leq pf \times S_{nom}, \quad (5)$$

$$-\sqrt{1 - pf^2} S_{nom} \leq Q_{DG} \leq \sqrt{1 - pf^2} S_{nom}. \quad (6)$$

4.2. Positive-sequence sensitivity impedance matrix

This study presents the following pseudo codes to build a three-

Table 4
Pseudo code 2. Finding a new bus that is connected to another bus.

```

nbs := no. of buses
for i := 1 to nbs
  if i != reference bus no.
    tmp := 0
    for j := 1 to nbr
      if tmp == 0
        n := starting bus, m := ending bus, and id := phase impedance matrix id
        if n != reference bus no.
          for k := 1 to nbs
            if k != i
              Zbus((k-1)×3+1:k×3, (i-1)×3+1:i×3) := Zbus((k-1)×3+1:k×3, (n-1)×3+1:n×3)
              Zbus((i-1)×3+1:i×3, (k-1)×3+1:k×3) := Zbus((k-1)×3+1:k×3, (n-1)×3+1:n×3)
            end
          end
          zb := Zabc((id-1)×3+1:id×3, 1:3)
          Zbus((i-1)×3+1:i×3, (i-1)×3+1:i×3) := Zbus((n-1)×3+1:n×3, (n-1)×3+1:n×3)+zb
          tmp := 1
        end
      end
    end
  end
end
end
end
end

```

phase sensitivity impedance matrix, Z_{bus} .

1) *Finding a bus that is connected to the reference.* A 3×3 phase impedance matrix of a bus that is directly connected to the reference bus is searched, as shown in the pseudo code in Table 3.

2) *Finding a bus that is connected to another bus.* When finding a new bus that is connected to the existing bus, Z_{bus} is revised, as shown in the pseudo code in Table 4.

For example, if the total number of buses is N , the proposed algorithms build an $(N \times 3)$ by $(N \times 3)$ Z_{bus} , which consists of phase impedance matrices (3×3 Z_{abc} , usually after Kron reduction). The sequence impedance is derived by

$$Z_{012} = T Z_{abc} T^{-1} = \begin{bmatrix} Z_{00} & Z_{01} & Z_{02} \\ Z_{10} & Z_{11} & Z_{12} \\ Z_{20} & Z_{21} & Z_{22} \end{bmatrix}. \quad (7)$$

In unbalanced systems, the mutual coupling components in (7) (i.e., Z_{01} , Z_{02} , and others) are not zero. However, they are sufficiently small to ignore if the system is not heavily unbalanced or is either fully or well transposed. Thus, the proposed method uses the positive-sequence impedance (i.e., Z_{11}) that regulates the average magnitude of the three-phase voltages as the sensitivity impedance matrix in (2)–(6).

$$Z_{bus,ij}^{pos} = Z_{012,ij}[2, 2], \quad (8)$$

$$Z_{012,ij} = T Z_{bus,ij} T^{-1}, \quad (9)$$

$$Z_{bus,ij} = Z_{bus}[(i-1) \times 3 + 1 : i \times 3, (j-1) \times 3 + 1 : j \times 3], \quad (10)$$

for $i = 1$ to N and $j = 1$ to N .

4.3. Verification of reactive power control

To validate the proposed three-phase Volt/Var control method, this study models a heavily unbalanced three-phase IEEE 34-bus test feeder and adds a 1-MVA PV system that can inject reactive power into the test feeder, as shown in Fig. 9. The feeder includes two voltage regulators, two shunt capacitors (on buses 844 and 848, which have a total capacity of 750 kVar), and six wye- or delta-connected constant power, current, and impedance loads (1047 kW and 677 kVar), and 19 wye- or delta-connected constant power, current, and impedance loads (722 kW and 367 kVar). The detailed system data can be found in [44,45]. The bus to which the PV system is connected shows the highest capacity among the distributed loads (i.e., the wye-connected constant power load on bus 822).

The positive-sequence sensitivity impedance matrix of the test feeder is determined by the pseudo codes in Table 3 and Table 4. Then, the reactive-power output of the PV system is determined by the iteration of Eqs. (2) to (5). To determine the maximum effect of Volt/Var control on voltage regulation, this study initially assumes that the PV system (a) actively controls reactive power and (b) can inject more reactive power than active power within the capability curve. That is, the power-factor limit is not set in the first verification study but will be set in the next verification study. Table 5 presents the phase and positive-sequence voltages after participating in Volt/Var control. The PV system successfully maintains the positive-sequence voltage magnitude of a bus to which the PV system is connected within the set voltage range (e.g., 1.0 p.u.). A positive sign for the active and reactive power means injecting active or reactive power, and a negative sign means absorbing these types of power. For example, the PV system (i.e., PV1) that is connected to bus 822 absorbs a reactive power of 995.04 kVar, regulating a positive-sequence voltage of $1.0158 \angle -2.40^\circ$ p.u. up to a set voltage of 1.00 p.u. (i.e., $1.000079 \angle -1.49^\circ$ p.u.) at a mismatch accuracy of $1e-4$. In fact, the PV system (i.e., PV1) absorbs the reactive power from the test feeder, so the reactive power at the slack bus (i.e., 800) increases from 252 kVar to 1313 kVar in Table 5.

As the next validation step, the positive-sequence voltage and quadrature current of bus 822 (i.e., PV1) are plotted in Figs. 10 and 11. Because the voltage and current converge to the set value, both figures can be seen as a validation of the proposed method.

One of the constraints of Volt/Var control for electric utilities is to keep the power factor at the slack bus close to unity, so DG (including PV) inverters that are connected to the grid should be coordinated with electric utilities. In fact, inverter-based DG systems often operate at a unity or fixed power factor [41]. Thus, the second validation study applies the power-factor limit (e.g., lagging power factor of 0.9) to the proposed Volt/Var-control method. Table 6 presents the phase and positive-sequence voltages after Volt/Var control for the proposed

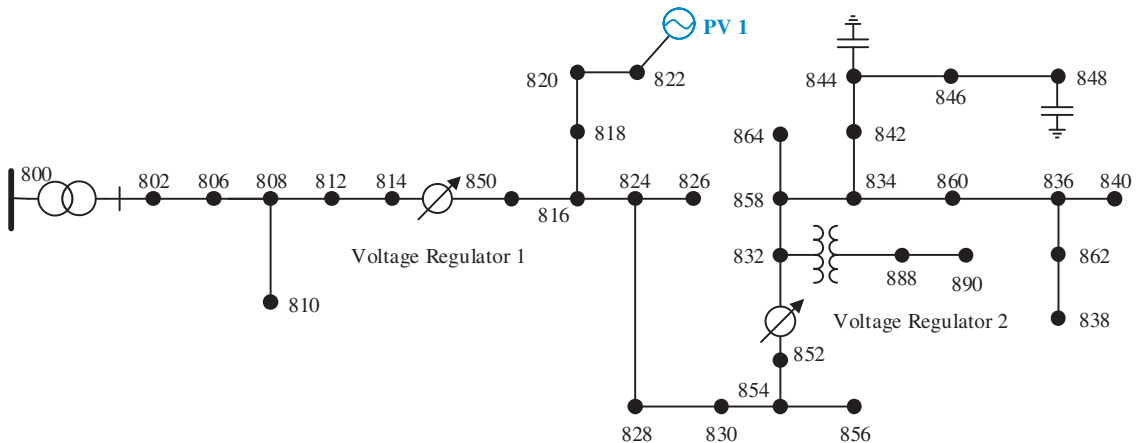


Fig. 9. IEEE 34-bus test feeder [44,45].

Table 5
Bus voltages after participating in Volt/Var control.

Bus	Phase	Before connecting PV		After connecting PV (Volt/Var control)		
		P + jQ in kVA		P + jQ in kVA		
Slack	Total	2041.21 + j252.34		2102.94 + j1313.09		
-	Bus voltage	Set		Voltage	Current	Complex power
Bus	Phase	p.u.	p.u.	p.u.	A	kVA
822	a	0.996690∠-2.47°	1.00	0.981853∠1.65°	23.09∠89.39°	12.86-325.60i
	b	1.031226∠-122.94°		1.015481∠-119.41°	23.09∠-31.37°	11.51-336.84i
	c	1.019403∠118.22°		1.002904∠122.22°	23.09∠-150.00°	12.87-332.60i
	Positive-sequence	1.015773∠-2.40°		1.000079∠1.49°	23.09∠89.34°	37.23-995.04i

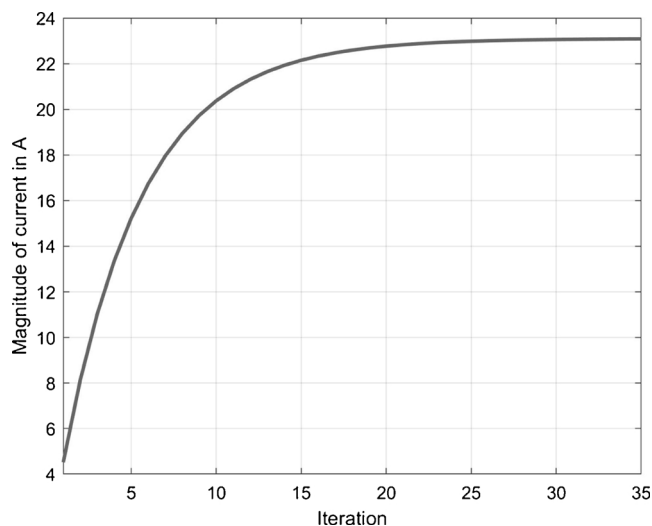


Fig. 10. Magnitude of the quadrature current that is produced in bus 822.

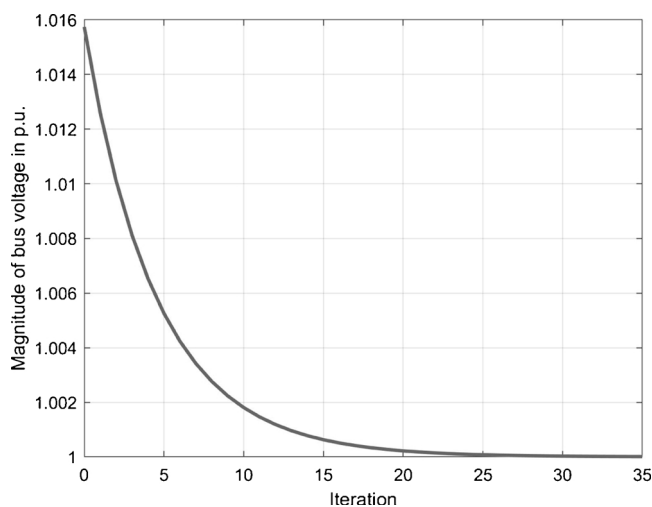


Fig. 11. Positive-sequence voltage of bus 822.

method. The proposed method attempts to inject reactive power to regulate the positive-sequence voltage magnitude within a set voltage, but the PV system violates the power factor limit of 0.9. Therefore, the proposed method sets the maximum reactive power that does not violate the power-factor limit. That is, the PV system absorbs a reactive power of 435.89 kVar. A positive sign for the active and reactive power means injecting active and reactive power, and a negative sign means absorbing these types of power. The active power at the slack bus (i.e., 800) decreases from 2041 kW to 1070 kW because the PV system injects 900 kW into the test feeder. In contrast, the reactive power at the slack bus increases from 252 kVar to 689 kVar in Table 6 because the PV

system absorbs the reactive power (i.e., 435.89 kVar). This study calculates the power flow of the test feeder with the backward and forward sweep algorithm, the detailed codes of which are found in the Appendix of Ref. [46].

5. Conclusions

The main objectives of this study were to (a) perform a case study to analyze the steady-state response of a large distribution network with 3434 buses when relatively moderate- and high-capacity renewable PV systems either produce or consume reactive power and (b) present a three-phase Volt/Var-control method. The first case study used OpenDSS to model an actual substation distribution system with 3434 buses, including feeder J1 and thirteen PV systems that could control Volt/Var. According to the case studies, high-capacity PV systems (i.e., 31.2% of total peak generation of the distribution system) that could not control Volt/Var increased overvoltage along the feeder. In contrast, high-capacity PV systems that could control Volt/Var mitigated such an increase in voltage. The first case study determined the reactive power by the relationship between the predefined slope and the bus voltage's current magnitude, ignoring the impedance sensitivity of the feeders. Thus, this study presented a three-phase Volt/Var-control method that could regulate the positive-sequence magnitude of three-phase voltages by using a positive-sequence sensitivity impedance matrix with power-factor constraints.

The verified three-phase Volt/Var-control method can be used for DG inverters to keep the average of the three-phase voltages within a set voltage range (e.g., the local feedback controller). The proposed method was also verified for unbalanced three-phase systems and can be included in various three-phase power-flow analysis programs (e.g., DIgSILENT and OpenDSS). The proposed methods can also examine the maximum effect of DG systems by controlling reactive power during voltage regulation. For example, the large feeder model with 3434 buses that was modeled in OpenDSS can be used for various impact-analysis studies of a distribution system with various inverter-based DG systems that can control reactive power, including wind farms and PV plants.

Conflict of interest

The authors declare that they have no known competing financial interests or personal relationships that could have appeared to influence the work reported in this paper.

Acknowledgments

The authors would like to thank (a) Yamille del Valle at the National Electric Energy Testing Research and Applications Center and Raey Regassa at the Georgia Institute of Technology for their input to discussions pertaining to the power-flow calculation of distribution networks and Volt/Var control and (b) EPRI for its publication of the feeders J1, K1, and M1 on their public domain for research studies.

Table 6
Bus voltages after participating in Volt/Var control with the power-factor limit.

Bus	Phase	Before connecting PV		After connecting PV (Volt/Var control)		
		P + jQ in kVA		P + jQ in kVA		
Slack	Total	2041.21 + j252.34		1070.12 + j689.30		
–		Bus voltage	Set	Voltage	Current	Complex power
Bus	Phase	p.u.	p.u.	p.u.	A	kVA
822	a	0.996690∠-2.47°	1.00	1.021558 ∠1.67°	22.70∠27.52°	300–145.30i
	b	1.031226∠-122.94°		1.051985 ∠-119.37°	22.04∠-93.53°	300–145.30i
	c	1.019403∠118.22°		1.043189 ∠122.14°	22.23∠147.98°	300–145.30i
	Positive-sequence	1.015773∠-2.40°		1.038911 ∠1.48°	22.32∠27.33°	900–435.89i

The authors gratefully acknowledge the support of the National Science Foundation of the United States under Grant #1232070, which was used for a portion of the work presented herein. Any opinions, findings, and conclusions or recommendations expressed in this material are those of the author(s) and do not necessarily reflect the views of the National Science Foundation. This research was supported by Korea Electric Power Corporation under Grant #1208200052.

References

- [1] ANSI C84.1-2016, American national standard for electric power systems and equipment—voltage ratings (60 Hz), National Electrical Manufacturers Association (2016).
- [2] "Voltage characteristics of electricity supplied by public distribution systems," European Committee for Electrotechnical Standardization, 2005.
- [3] IEEE Std 1547a-2014 (Amendment to IEEE Std 1547-2003), IEEE Standard for Interconnecting Distributed Resources With Electric Power Systems - Amendment 1, (2014).
- [4] IEC 61727, Photovoltaic (PV) Systems - Characteristics of the Utility Interface, (2004).
- [5] C.F. Jack, Peak shaving—a way to fight rising costs, *IEEE Trans. Ind. Appl.* IA-12 (1976) 486–491.
- [6] F. Kamyab, M. Amini, S. Sheykha, M. Hasanpour, M.M. Jalali, Demand response program in smart grid using supply function bidding mechanism, *IEEE Trans. Smart Grid* 7 (2016) 1277–1284.
- [7] R.C. Dugan, T.E. McDermott, Distributed generation, *IEEE Ind. Appl. Mag.* 8 (2002) 19–25.
- [8] T. Ackermann, G. Andersson, L. Söder, Distributed generation: a definition, *Electr. Power Syst. Res.* 57 (2001) 195–204.
- [9] F. Katiraei, J.R. Agüero, Solar PV integration challenges, *IEEE Power Energy Mag.* 9 (2011) 62–71.
- [10] H.M. Ayres, W. Freitas, M.C. de Almeida, L.C.P. da Silva, Method for determining the maximum allowable penetration level of distributed generation without steady-state voltage violations, *IET Gener. Transm. Distrib.* 4 (2010) 495–508.
- [11] F.J. Ruiz-Rodríguez, J.C. Hernández, F. Jurado, Probabilistic load flow for photovoltaic distributed generation using the Cornish–Fisher expansion, *Electr. Power Syst. Res.* 89 (2012) 129–138.
- [12] E.N.M. Silva, A.B. Rodrigues, M. da Guia Da Silva, Stochastic assessment of the impact of photovoltaic distributed generation on the power quality indices of distribution networks, *Electr. Power Syst. Res.* 135 (2016) 59–67.
- [13] J. Driesen, R. Belmans, Distributed generation: challenges and possible solutions, in *IEEE Power Engineering Society General Meeting*, Montreal, Canada, 2006.
- [14] S.K. Solanki, V. Ramachandran, J. Solanki, Steady state analysis of high penetration PV on utility distribution feeder, in *2012 IEEE Transmission and Distribution Conference and Exposition*, Orlando, FL, USA, 2012.
- [15] K.G. Boroojeni, M.H. Amini, A. Nejadpak, S.S. Iyengar, B. Hoseinzadeh, C.L. Bak, A theoretical bilevel control scheme for power networks with large-scale penetration of distributed renewable resources, in *2016 IEEE International Conference on Electro Information Technology*, University of North Dakota, Grand Forks, ND, USA, 2016, pp. 0510–0515.
- [16] M.H. Amini, B. Nabi, M.R. Haghifam, Load management using multi-agent systems in smart distribution network, in *2013 IEEE Power & Energy Society General Meeting*, Vancouver, Canada, 2013.
- [17] A. Hoke, R. Butler, J. Hambrick, B. Kroposki, Steady-state analysis of maximum photovoltaic penetration levels on typical distribution feeders, *IEEE Trans. Sustain. Energy* 4 (2013) 350–357.
- [18] F. Lamberti, V. Calderaro, V. Galdi, G. Graditi, Massive data analysis to assess PV/ESS integration in residential unbalanced LV networks to support voltage profiles, *Electr. Power Syst. Res.* 143 (2017) 206–214.
- [19] P.M.S. Carvalho, P.F. Correia, L.A.F.M. Ferreira, Distributed reactive power generation control for voltage rise mitigation in distribution networks, *IEEE Trans. Power Syst.* 23 (2008) 766–772.
- [20] J. Smith, B. Seal, W. Sunderman, R. Dugan, Simulation of solar generation with advanced volt-var control, in *21th International Conference on Electricity Distribution*, Frankfurt, Germany, 2011.
- [21] J. Smith, Stochastic analysis to determine feeder hosting capacity for distributed solar PV, *Electric Power Research Institute* (2012).
- [22] J. Smith, Modeling High-Penetration PV for Distribution Interconnection Studies, *Electric Power Research Institute*, 2013.
- [23] R. Yan, T.K. Saha, Investigation of voltage stability for residential customers due to high photovoltaic penetrations, *IEEE Trans. Power Syst.* 27 (2012) 651–662.
- [24] K. Turitsyn, P. Sulc, S. Backhaus, M. Chertkov, Options for control of reactive power by distributed photovoltaic generators, *Proc. IEEE* 99 (2011) 1063–1073.
- [25] I. Roytelman, B.K. Wee, R.L. Lugtu, Volt/var control algorithm for modern distribution management system, *IEEE Trans. Power Syst.* 10 (1995) 1454–1460.
- [26] B.A. de Souza, A.M.F. de Almeida, Multiobjective optimization and fuzzy logic applied to planning of the volt/Var problem in distributions systems, *IEEE Trans. Power Syst.* 25 (2010) 1274–1281.
- [27] S. Genc, M. Baggu, Look ahead Volt/Var control: a comparison of integrated and coordinated methods, in *2014 IEEE PES T&D Conference and Exposition*, Chicago, USA, 2014.
- [28] J. Renedo, A. García-Cerrada, L. Rouco, Active power control strategies for transient stability enhancement of AC/DC grids with VSC-HVDC multi-terminal systems, *IEEE Trans. Power Syst.* 31 (2016) 4595–4604.
- [29] H. Zhao, Q. Wu, Q. Guo, H. Sun, Y. Xue, Optimal active power control of a wind farm equipped with energy storage system based on distributed model predictive control, *IET Gener. Transm. Distrib.* 10 (2016) 669–677.
- [30] A. Mitra, D. Chatterjee, Active power control of DFIG-based wind farm for improvement of transient stability of power systems, *IEEE Trans. Power Syst.* 31 (2016) 82–93.
- [31] D. Stimoniaris, D. Tsiamitros, E. Dialynas, Improved energy storage management and PV-active power control infrastructure and strategies for microgrids, *IEEE Trans. Power Syst.* 31 (2016) 813–820.
- [32] G. Chen, F.L. Lewis, E.N. Feng, Y. Song, Distributed optimal active power control of multiple generation systems, *IEEE Trans. Ind. Electron.* 62 (2015) 7079–7090.
- [33] T. Niknam, A.M. Ranjbar, A.R. Shirani, A. Ostadi, A new approach based on ant colony algorithm to distribution management system with regard to dispersed generation, in *18th International Conference and Exhibition on Electricity Distribution*, Turin, Italy, 2005.
- [34] S. Auchariyamet, S. Sirisumrannukul, Optimal daily coordination of Volt/Var control devices in distribution systems with distributed generators, in *45th International Universities Power Engineering Conference*, Cardiff, United Kingdom, 2010.
- [35] I. Kim, R.G. Harley, R. Regassa, Optimal distributed generation allocation on distribution networks at peak load and the analysis of the impact of volt/var control on the improvement of the voltage profile, in *2014 North American Power Symposium*, Pullman, WA, USA, 2014.
- [36] I. Kim, Optimal distributed generation allocation for reactive power control, *IET Gener. Transm. Distrib.* 11 (2017) 1549–1556.
- [37] Electric Power Research Institute. Distributed PV monitoring and feeder analysis. Available: <http://dpv.epri.com/>.
- [38] Electric Power Research Institute. Smart grid resource center. Available: <http://www.smartgrid.epri.com/SimulationTool.aspx>.
- [39] IEEE application guide for IEEE Std 1547(TM), IEEE Standard for Interconnecting Distributed Resources With Electric Power Systems, (2009).
- [40] Electric Power Research Institute, "Feeder J1," 2014.
- [41] IEEE Std 1547.7-2013, IEEE Guide for Conducting Distribution Impact Studies for Distributed Resource Interconnection, (2014).
- [42] R.C. Dugan, R.F. Arritt, J. Smith, M. Rylander, OpenDSS Training Workshop, University of North Carolina at Charlotte, 2013.
- [43] C.S. Cheng, D. Shirmohammadi, A three-phase power flow method for real-time distribution system analysis, *IEEE Trans. Power Syst.* 10 (1995) 671–679.
- [44] W.H. Kersting, Radial distribution test feeders, *IEEE Trans. Power Syst.* 6 (1991) 975–985.
- [45] IEEE PES AMPS DSAS Test Feeder Working Group. (August 2019). Distribution test feeders. Available: [sites.ieee.org/pes-testfeeders/resources/](https://www.ieee.org/pes-testfeeders/resources/).
- [46] I. Kim, Impact of Stochastic Renewable Distributed Generation on Urban Distribution Networks, Doctor of Philosophy, Electrical and Computer Engineering, Georgia Institute of Technology, 2014.